Surface-normal emission of a high-Q resonator using a subwavelength high-contrast grating

Ye Zhou, Michael Moewe, Johannes Kern, Michael C. Y. Huang, and Connie J. Chang-Hasnain

Department of Electrical Engineering and Computer Sciences, University of California, Berkeley, California 94720
cch@eecs.berkeley.edu

Abstract: We report a novel high-quality (Q) factor optical resonator using a subwavelength high-contrast grating (HCG) with in-plane resonance and surface-normal emission. We show that the in-plane resonance is manifested is by a sharp, asymmetric lineshape in the surface-normal reflectivity spectrum. The simulated Q factor of the resonator is shown to be as high as 500,000. A HCG-resonator was fabricated with an InGaAs quantum well active region sandwiched in-between AlGaAs layers and a Q factor of >14,000 was inferred from the photoluminescence linewidth of 0.07 nm, which is currently limited by instrumentation. The novel HCG resonator design will serve as a potential platform for many devices including surface emitting lasers, optical filters, and biological or chemical sensors.

OCIS codes: (050.2770) Gratings; (230.5750) Resonators

References and Links

1. D. Armani, T. Kippenberg, S. Spillane, and K. Vahala, "Ultra-high-Q toroid microcavity on a chip," Nature **421**, 925-928 (2003).
2. T. Asano, B.-S. Song, Y. Akahane, and S. Noda, "Ultrahigh-Q nanocavities in two-dimensional photonic crystal slabs," IEEE J. Sel. Top. Quantum Electron. **12**, 1121-1134 (2006).
3. D. Ohnishi, T. Okano, M. Imada, and S. Noda, "Room temperature continuous wave operation of a surface-emitting two-dimensional photonic crystal diode laser," Opt. Express **12**, 1562-1568 (2004).
4. W.-H. Chang, W.-Y. Chen, H.-S. Chang, T.-P. Hsieh, J.-I. Chyi, and T.-M. Hsu, "Efficient single-photon sources based on low-density quantum dots in photonic-crystal nanocavities," Phys. Rev. Lett. **96**, 117401-1-117401-4 (2006).
5. H. Takano, Y. Akahane, T. Asano, and S. Noda, "In-plane-type channel drop filter in a two-dimensional photonic crystal slab," Appl. Phys. Lett. **84**, 2226-2228 (2004).
6. E. Chow, A. Grot, L. Mirkarimi, M. Sigalas, and G. Girolami, "Ultracompact biochemical sensor built with two-dimensional photonic crystal microcavity," Opt. Lett. **29**, 1093-1095 (2004).
7. J. Niehusmann, A. Vörckel, P. H. Bolivar, T. Wahlbrink, W. Henschel, and H. Kurz, "Ultrahigh-quality-factor silicon-on-insulator microring resonator," Opt. Lett. **29**, 2861-2863 (2004).
8. A. Loffler, J. Reithmaier, G. Sek, C. Hofmann, S. Reitzenstein, M. Kamp, and A. Forchel, "Semiconductor quantum dot microcavity pillars with high-quality factors and enlarged dot dimensions," Appl. Phys. Lett. **86**, 111105 (2005).
9. H. A. Haus and Y. Lai, "Narrow-band distributed feedback reflector design," J. Lightwave Technol. **9**, 754-760 (1991).
10. R. Magnusson and S. Wang, "New principle for optical filters," Appl. Phys. Lett. **61**, 1022-1024 (1992).
11. S. Peng and G. M. Morris, "Experimental demonstration of resonant anomalies in diffraction from two-dimensional gratings," Opt. Lett. **21**, 549-551 (1996).
12. M. Neviere, R. Petit and M. Cadilhac, "About the theory of optical crating coupler-waveguide systems," Opt. Commun. **8**, 113-117 (1973).
13. C. F. R. Mateus, M. C. Y. Huang, J. E. Foley, P. R. Beatty, P. Li, B. T. Cunningham, and C. J. Chang-Hasnain, "Compact label-free biosensor using VCSEL-based measurement system," IEEE Photon. Technol. Lett. **16**, 1712 (2004).
14. M. Lu, S. S. Choi, C. J. Wagner, J. G. Eden and B. T. Cunningham, "Label free biosensor incorporating a replica-molded, vertically emitting distributed feedback laser" Appl. Phys. Lett. **92**, 261502 (2008).
15. C. F. R. Mateus, M. C. Y. Huang, D. Yunfei, A. R. Neureuther, and C. J. Chang-Hasnain, "Ultrabroadband mirror using low-index cladded subwavelength grating," IEEE Photon. Technol. Lett. **16**, 518-520 (2004).
16. M. C. Y. Huang, Y. Zhou, and C. J. Chang-Hasnain, "A surface-emitting laser incorporating a high-index-contrast subwavelength grating," Nat. Photonics **1**, 119-122 (2007).

#100263 - $15.00 USD Received 18 Aug 2008; revised 6 Oct 2008; accepted 6 Oct 2008; published 13 Oct 2008

17. L. Ferrier, S. Boutami, F. Mandorlo, X. Letartre, P. Rojo Romeo, P. Viktorovitch,P. Gilet, B. B. Bakir, P. Grosse, J.-M. Fedeli,A. Chelnokov, "Vertical microcavities based on photonic crystal mirrors for III-V/Si integrated microlasers," Proc. SPIE. **6989**, 69890W (2008).
18. M. C. Y. Huang, Y. Zhou, and C. J. Chang-Hasnain, "A nanoelectromechanical tunable laser," Nat. Photonics **2**, 180-184 (2008).
19. M. G. Moharam and T. K. Gaylord, "Rigorous coupled-wave analysis of planar-grating diffraction," J. Opt. Soc. Am. **71**, 811-818 (1981).
20. S. H. Fan, W. Suh, and J. D. Joannopoulos, "Temporal coupled-mode theory for the Fano resonance in optical resonators," J. Opt. Soc. Am. A **20**, 569-572 (2003).
21. J. P. Kim and A. M. Sarangan, "Temperature-dependent Sellmeier equation for the refractive index of AlxGa1-xAs," Opt. Lett. **32**, 536 (2007).

1. Introduction

High-quality (Q) factor optical resonators have attracted much attention with various applications including lasers, single photon sources, optical filters, and sensors [1-6]. Various structures have been used to form high-Q resonators including microdisks, photonic crystals, ring resonators, distributed Bragg reflectors (DBRs) and distributed feedback (DFB) structures [1,2,7-9]. Most of them employ a collinear configuration for the resonant optical mode and optical output. While such configuration facilitates device integration in a cascaded fashion, it does not facilitate simple coupling with fiber or free-space optics. A high-Q resonator with surface-normal emission is of great interest in many applications such as lasers, optical filters and sensors.

Anomalies in periodically modulated grating structures have been widely studied [10-12]. It has been shown that gratings with a subwavelength modulation in refractive index can function as filters due to the guided-mode resonance [12]. This resonance has been successfully exploited in the development of some sensor applications [13,14]. However, the refractive index modulations in most pervious gratings are relatively weak. Recently, we proposed a novel subwavelength high-index-contrast grating (HCG) as a broadband reflector for an optical beam propagating in the direction perpendicular to the grating plane [15]. The very large periodic index contrast from the gratings in the in-plane direction results in an efficient coupling of the surface-normal waves with the in-plane waves and, hence, yields ultrahigh reflectivity over a broad spectrum. It has been shown that HCG can replace conventional DBR structure as an alternative solution for vertical cavity surface emitting laser (VCSEL) mirrors [16,17]. We further demonstrated tunable VCSELs with a HCG as a movable reflector [18].

In this work, we present a completely new high-Q resonator configuration using the high contrast grating. In particular, the in-plane high-contrast grating is designed to form a high-Q resonator. In addition, it couples light in the surface-normal direction. We present a design with the Q factor as high as 500,000 using the finite difference-time-domain (FDTD) numerical simulation. Experimentally, we designed and fabricated HCG-resonator (HCG-R) structures on a wafer consisting of InGaAs quantum wells sandwiched in-between AlGaAs layers. In contrast with the typical 20 nm wide photoluminescence (PL) spectrum, a very narrow band of 0.07 nm is obtained with the HCG-R structure, of which the measurement is limited by our instrumentation. A very high Q factor of 14,000 is inferred from this data. A much higher Q is expected with optimization of fabrication and characterization system. The unique feature of high-Q with surface-normal emission is highly desirable as the unique topology facilitates convenient and high output coupling with free-space or fiber optics. This feature is promising for array fabrication of lasers and filters, as well as high throughput sensor arrays.

2. Design and theoretical simulation

The schematic of an infinite HCG structure is shown in Fig. 1(a), with stripes that are periodic in the x direction and are infinite in both the x and y directions. The high-index material, which is freely suspended and fully surrounded by air as the low-index material, consists of $Al_{0.6}Ga_{0.4}As$ with three $In_{0.2}Ga_{0.8}As$ quantum wells embedded inside as an active material. The

#100263 - $15.00 USD Received 18 Aug 2008; revised 6 Oct 2008; accepted 6 Oct 2008; published 13 Oct 2008

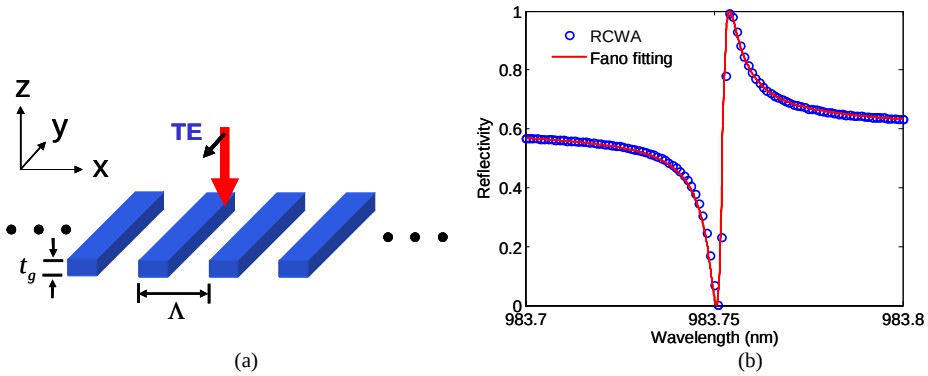

(a) (b)

Fig. 1. (a). Schematic of a HCG structure (b). Simulated reflectivity spectrum of HCG grating using RCWA shown in blue circles. Red curve is the fitted Fano resonance line shape. Q factor is ~500,000

reflectivity spectrum of the resonator is calculated using Rigorous Coupled Wave Analysis (RCWA) [19] for a normal-incident TE-polarized plane wave with its electric field parallel to the gratings, shown as blue circles in Fig. 1(b). The grating is specified by three parameters: the period (Λ), thickness (t_g), and duty cycle (η). Duty cycle is defined as the ratio of the width of the high index material to Λ. Choosing the appropriate parameters, we can obtain a reflectivity spectrum with a sharp asymmetric line shape whose reflectivity varies from 0 to 1 over a very narrow wavelength range. In this case, Λ= 484 nm, t_g= 390 nm, and η= 64%. This asymmetric resonance has been reported previously for photonic crystals and is referred to as Fano resonance [20]. It is the result of the interference between the normal incidence beam and the in-plane resonance of the HCG. The Q factor of the resonance can be extracted by fitting the simulated reflectivity spectrum with following Fano-resonance equation [20]:

$$R = \frac{r^2(\omega-\omega_0)^2 + t^2(1/\tau)^2 - 2rt(\omega-\omega_0)(1/\tau)}{(\omega-\omega_0)^2 + (1/\tau)^2} \quad (1)$$

where ω_0 and τ are the center frequency and the lifetime of the resonance; r and t are the electric field reflectivity and transmittance of a uniform slab with the same thickness as the HCG layer and with an effective dielectric constant. The Q factor of the resonance can be calculated using $Q = \omega_0 \tau$. The red curve in Fig. 1(b) shows the fitted Fano-resonance curve based on Eq. (1). The extracted Q factor in this case is calculated to be ~500,000.

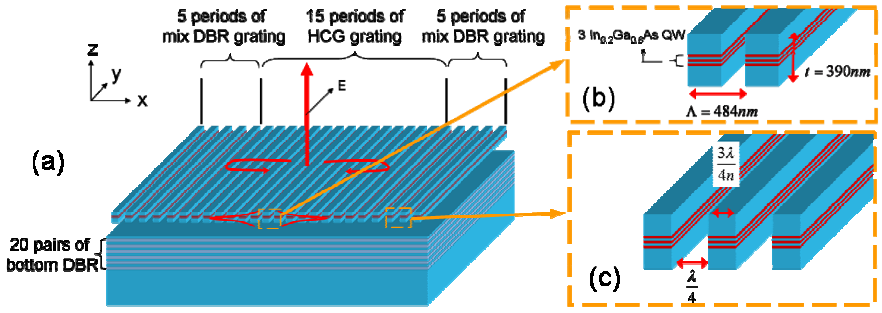

Fig. 2. (a). Schematic of HCG high-Q resonator. (b) Schematic of middle HCG grating with three $In_{0.2}Ga_{0.8}As$ quantum wells embedded inside grating layer. (c) Schematic of side mix-DBR grating mirror which is a combination of 1st-order and 3rd-order DBR gratings.

For device applications, however, it is essential to consider a finite sized HCG. To prevent light leakage from all four symmetric directions, i.e. ±x and ±z, we considered a structure with distributed Bragg reflectors (DBRs) at the ±x ends and below the HCG, as shown in Fig. 2. In

#100263 - $15.00 USD Received 18 Aug 2008; revised 6 Oct 2008; accepted 6 Oct 2008; published 13 Oct 2008

this structure, the HCG grating consists of n-period gratings with three $In_{0.2}Ga_{0.8}As$ quantum wells sandwiched between $Al_{0.6}Ga_{0.4}As$ layers, as shown in Fig. 2(b), where n varies from 3 to 15. The end-DBRs are a combination of 1st-order DBR gratings and 3rd-order DBR gratings for ease of fabrication, as shown in Fig. 2(c). The bottom-DBR consists of 20 pairs of λ/4-thick AlAs/GaAs layers grown on the substrate.

Figure 3(a) shows the numerical simulation result of the field intensity profile in the HCG high-Q resonator using the finite-difference time-domain (FDTD) method. In the calculation, a TE-polarized (electric field parallel with the grating) dipole source is excited in the center of the HCG resonator for a short period of time. After the dipole source is terminated, the electric field intensity profile of the resonator is monitored and recorded. The simulation shows that energy can be well-confined inside the HCG resonator and the output light only emits in the surface-normal direction. Figure 3(b) shows the electric field intensity inside the resonator as a function of time after the excitation is turned off. Devices with different numbers of HCG periods are simulated. As shown in Fig. 3(b), electric field intensity decays exponentially with time. Based on this decay rate, the Q factor of the resonance can be calculated. For the devices with 3, 5, 7 and 15 periods of HCG, the Q factor is calculated to be 900, 4000, 17000 and 500,000 respectively. Next, optical gain is incorporated into the $In_{0.2}Ga_{0.8}As$ quantum wells in the FDTD simulation. Assuming the grating material is lossless, the threshold gain required in the quantum well for lasing is as low as 30 cm^{-1} for the high-Q resonator design with 15 periods of HCG.

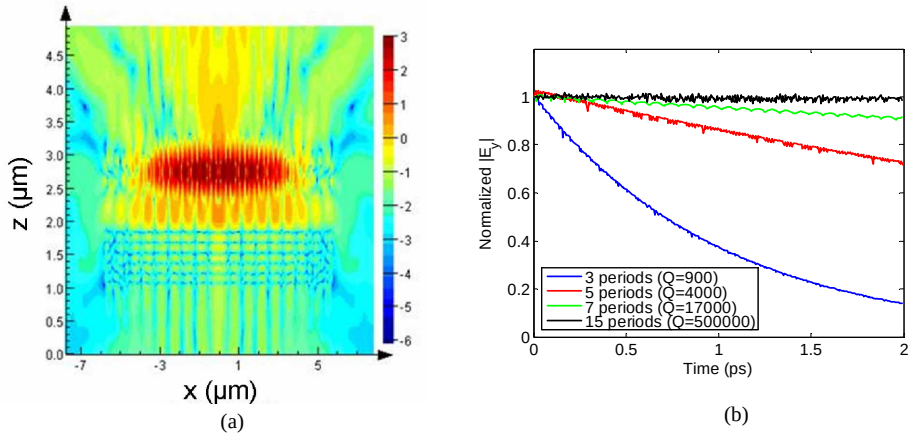

(a) (b)

Fig. 3. (a). Simulated electric field intensity profile in the HCG resonator. Color is labeled in log scale. Q is estimated to be 500,000. (b) Normalized electrical field decay as a function of time in the HCG resonator for different number of HCG periods (3 periods, 5 periods, 7 periods and 15 periods). Q is estimated to be 900, 4000, 17000 and 500000 respectively.

The HCG resonant wavelength as a function of grating dimensions and refractive indices is also studied. It is interesting to note that the wavelength peak can be designed to be highly sensitive to the thickness of an extra layer deposited on the HCG. However, the wavelength and Q value are highly insensitive to the HCG index or temperature variations. These attributes make the HCG-R highly desirable for sensors and uncooled optoelectronic device applications, respectively.

The HCG we simulated has dimensions Λ, t_g, and η equal to 502 nm, 385 nm, and 64%, respectively. The refractive indices of the high and low index materials are 3.15 and 1, respectively. Figure 4(a) shows the calculated spectra of a HCG having various thickness of refractive index of 1.3 material deposited on it. The HCG wavelength increases greatly with deposited material at a rate of 0.44 nm/nm, which is significantly larger than the 0.27 nm/nm obtained for guided-mode resonator sensors [13]. This large sensitivity is due to the high index contrast of the HCG grating and a larger overlap of optical field with the biomaterials,

#100263 - $15.00 USD Received 18 Aug 2008; revised 6 Oct 2008; accepted 6 Oct 2008; published 13 Oct 2008

which can be wrapped around the gratings in an HCG-R. In addition, the linewidth remains small due to the high Q value. Both factors will contribute to a rapid and easy detection of small thickness changes.

For applications such as lasers and filters, it is desirable for the resonant wavelength and Q value to be temperature insensitive. Figure 4(b) shows the simulation results for HCG resonant wavelength and Q factor as a function of temperature. The refractive index temperature dependence of the grating material is assumed to be 2×10^{-4}/K [21]. Figure 4(b) shows that the HCG based laser resonant wavelength shifts only 0.5 Å/K and the Q factor of the HCG cavity remains almost constant when temperature is changed from 0 ˚C to 100 ˚C. As a comparison, the emission wavelength shifts 1 Å/K in a DBR laser or VCSEL, and 3 Å/K for a Fabry-Perot laser. This improvement in the temperature stability mainly comes from the large index contrast with a low index material whose refractive index does not change when temperature is changed.

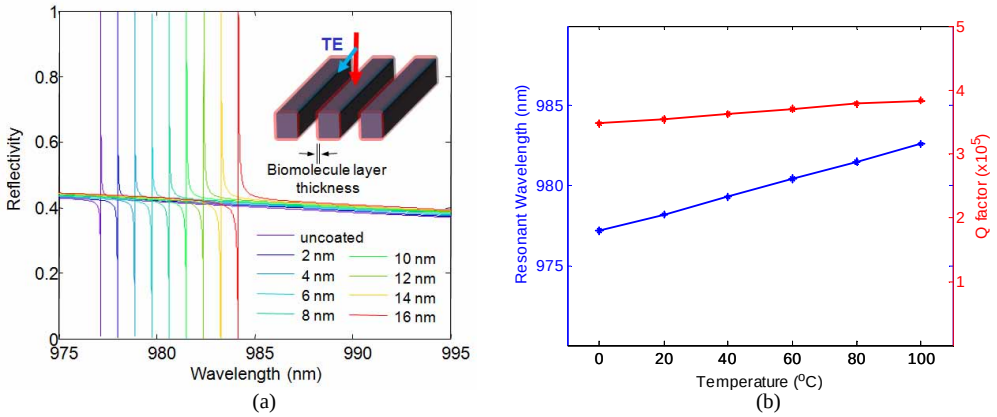

Fig. 4. (a). Simulation results for a HCG biosensor. The resonant wavelength red shift when biomolecule layers with different thicknesses are deposited onto the HCG structure. (b). Simulation results for HCG resonant wavelength and Q factor as a function of temperature. Resonant wavelength only shifts 0.5 Å/K and the Q factor of the HCG cavity remains almost constant when temperature is changed from 0 ˚C to 100 ˚C.

3. Experimental results

The proposed HCG high-Q resonator is experimentally demonstrated. The device was grown by metal organic chemical vapor deposition (MOCVD) on a GaAs substrate. The grating structure was patterned by electron-beam lithography on poly-methyl methacrylate (PMMA) photoresist and then etched by reactive ion etching (RIE). A wet chemical-based selective etching followed by critical point drying was used to remove the sacrificial material underneath the HCG layer and form the freely suspended grating. Figure 5 shows the scanning

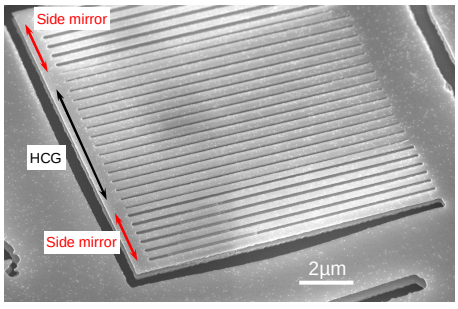

Fig. 5. SEM image of fabricated HCG high-Q resonator.

#100263 - $15.00 USD Received 18 Aug 2008; revised 6 Oct 2008; accepted 6 Oct 2008; published 13 Oct 2008

electron microscopy (SEM) image of a fabricated HCG high-Q resonator with center HCG labeled in black and side mix-DBR mirror labeled in red.

Low-temperature (4K) PL was measured using a Ti:Sapphire laser at 800 nm wavelength. The emission spectrum of the wafer without the HCG-R structure is plotted in blue in Fig. 6(a) showing a typical PL spectrum of the InGaAs quantum wells with a full-width half-maximum (FWHM) linewidth of 20 nm. The HCG resonator emission is shown as the red curve in Fig. 6(a). A very narrow PL emission linewidth is obtained. The inset shows the zoomed-in emission with a FWHM linewidth as narrow as 0.07 nm, which is limited by our spectrometer resolution. This translates to a Q factor as high as 14,000. Figure 6(b) shows the PL emission spectra under different pumping levels. With increasing pumping power, no further narrowing of the spectrum was observed, most likely due to our instrumentation limitation. Future experiments will include measurements with improved resolution and time-resolved PL.

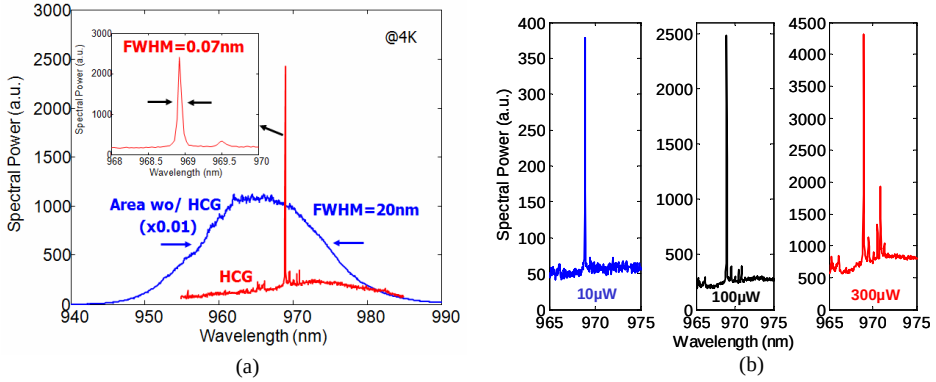

Fig. 6. (a). Emission spectrum of HCG resonator (in red) and emission spectrum in the area without grating (in blue). The inset shows a zoomed-in picture of the HCG emission spectrum. The FWHM of the HCG resonator emission peak is ~0.07nm and Q is ~14000. (b) Emission spectra of HCG resonator under 10μW, 100μW, 300μW optical pumping, respectively.

4. Conclusion

We presented a high-Q resonator structure using a high contrast subwavelength grating for the first time. A Q factor of ~500,000 was obtained by numerical simulation. In addition, we show a very high sensitivity of the wavelength peak to the thickness of material coated on the HCG. This topology makes the device an excellent candidate for high throughput sensing of biological or chemical agents. The Q value and wavelength are insensitive to temperature variation, making them well suited for uncooled device applications. Finally, a Q value of 14,000 is experimentally demonstrated by the PL of an HCG-R with inclusion of an active quantum well region.

The HCG resonator proposed here has many desirable attributes that lends itself to being an excellent platform for devices such as lasers, modulators, detectors, filters, and sensors. First, the epitaxial structure is very thin, which significantly relaxes the stringent requirements typically found in thick epitaxy (several microns) used for optoelectronic devices. Therefore, it may open the door for devices in a wavelength regime where epitaxy presents a major challenge. Secondly, the surface-normal emission facilitates simple and high efficiency output coupling for free-space or fiber optics. Finally, this structure facilitates scalability. By expanding the grating size, it is easy to increase the Q or tailor a designable passband for filters by inclusion of sections of HCGs with different dimensions.

Acknowledgments

We thank LandMark Optoelectronic Corporation for the growth of epitaxy wafers and Berkeley Microfabrication Laboratory for the fabrication support.

#100263 - $15.00 USD Received 18 Aug 2008; revised 6 Oct 2008; accepted 6 Oct 2008; published 13 Oct 2008